

RESEARCH

Open Access



Micro-XCT analysis of anatomical features and dimensions of the incisive canal: implications for dental implant treatment in the anterior maxilla

Vladimir S. Todorovic^{1,2*} , Mia-Michaela Beetge³ , Judy Kleyn⁴ , Jakobus Hoffman⁵  and Andre W. van Zyl⁶ 

Abstract

Background This study used micro-focus X-ray Computed Tomography (micro-XCT) to examine the anatomical differences and dimensions of the maxillary incisive canal (MIC) in a South African population. The accurate imaging yielded dependable results that support earlier research and enhance anterior maxilla surgery planning. Furthermore, these anatomical features are compared between various racial and gender groupings in the study.

Methods Using a micro-XCT scanner, 108 human cadaver skulls from the Pretoria Bone Collection were scanned and included in the study. Advanced volume rendering software was employed for measuring the MIC length, diameter, shape, and the buccal bone wall measurements in relation to the MIC.

Results Significant anatomical variation in the size and shape of the MIC was identified in the population, with variations seen between racial and gender groups. The incisive foramen (ICO) mean diameter was 6.61 mm, and the MIC length varied from 4.96 to 20.10 mm. There were significant differences in the buccal alveolar bone height between different ethnic groups and gender. Regarding morphological patterns in coronal and sagittal views, single canals were more common in the black population while Y-shaped canals were more common in the white population. The study also introduced a new metric by measuring the mean distances between teeth #11 and #21 and the ICO (1.83 mm and 1.88 mm respectively).

Conclusions The complex anatomical differences of the MIC in a South African population were clarified. Clinicians should be aware of tooth sockets in near proximity to the MIC and perform accurate preoperative assessment using sophisticated 3-D imaging and preferable guided implant placement in the anterior maxilla.

Keywords Micro-XCT, Dental implants, Maxillary bone, Anatomy, Maxillary incisive canal

*Correspondence:

Vladimir S. Todorovic
todent@yahoo.com

¹School of Dental Medicine, University of Belgrade, Belgrade
11000, Serbia

²Department of Periodontics and Oral Medicine, Faculty of Health
Sciences, University of Pretoria, Pretoria, South Africa

³Head Clinical Unit, Department of Periodontics and Oral Medicine,
Faculty of Health Sciences, University of Pretoria, Pretoria, South Africa

⁴Department of Statistics, Faculty of Natural and Agricultural Sciences,
University of Pretoria, Pretoria, South Africa

⁵Necsa (The South African Nuclear Energy Corporation), Pretoria, South
Africa

⁶Private Practice, Western Cape, South Africa



© The Author(s) 2024. **Open Access** This article is licensed under a Creative Commons Attribution 4.0 International License, which permits use, sharing, adaptation, distribution and reproduction in any medium or format, as long as you give appropriate credit to the original author(s) and the source, provide a link to the Creative Commons licence, and indicate if changes were made. The images or other third party material in this article are included in the article's Creative Commons licence, unless indicated otherwise in a credit line to the material. If material is not included in the article's Creative Commons licence and your intended use is not permitted by statutory regulation or exceeds the permitted use, you will need to obtain permission directly from the copyright holder. To view a copy of this licence, visit <http://creativecommons.org/licenses/by/4.0/>.

Introduction

Clinical anatomy represents the foundation for surgical interventions and forms the basis for diagnosis, treatment, and aftercare [1]. Anatomical differences between individuals are well-documented and can influence clinical outcomes. Failure to consider these variations may result in atypical symptom presentations, which can complicate clinical examinations and the interpretation of imaging results [2]. Intra- and post-operative complications, such as lack of dental implant osseointegration, nerve damage, and poor prosthodontic outcomes can all result from inadequate anatomical awareness [1, 3–6]. Therefore, it is crucial to have a comprehensive knowledge of clinical anatomy and any potential individual anatomical differences to execute safe and successful oral surgical procedures such as implant placement and application of local anaesthetic in the anterior maxilla [1, 7, 8].

The maxillary incisive canal (MIC), also called in the literature the nasopalatine canal (NC) or anterior palatine canal, has been described as a canal located in the middle of the palate, posterior to the roots of the central maxillary incisors [4, 7, 9, 10]. To define the terminology adequately and avoid any confusion, this study will employ the nomenclature established by Song and colleagues (2009): (1) the canal is referred to as the MIC (nasopalatine canal is another term used that is anatomically correct); (2) the inferior opening known as the incisive foramen (ICO) and; (3) the superior opening is referred to as either the nasal opening(s) (ICN) or the foramen of Stenson [11]. The ICO is typically found directly beneath the incisive papilla in the midline of the anterior palate [9]. The MIC is an important connection between the nasal and oral cavities, containing the nasopalatine nerve, descending branch of nasopalatine artery, fibrous connective tissue, and minor salivary glands [4, 7, 10]. The morphology and size of the MIC have been reported by a number of researchers [1, 4–6, 8–10, 12–16]. The MIC can have up to four canals in the midline, two to five ICN's and one to three ICO's [3, 5, 11, 17]. Sicher and colleagues (1962) reported up to six separate ICN's [18]. When there are many foramina, it is thought that the neural and vascular components are also divided [6, 18]. In order to prevent harming the neurovascular systems in the MIC and subsequent osseointegration failure, dental implant placement should protect all neural canaliculi [3]. Bilateral canals with openings on either side of the palatal incisive papilla are rare and is more prevalent in other mammals, such baboons or dogs, and is linked to the Jacobson accessory vomeronasal organs, which have smell and taste receptors [19].

Previous studies have revealed differences in the MIC size and morphology, as well as the thickness of the anterior maxilla bone in relation to age, gender, edentulism, and ethnicity [5, 7–13, 20, 21]. In the dentulous maxilla,

the typical MIC diameter is less than 6 mm; if this value is exceeded, conditions including canal cysts, trauma, and tooth loss may be present [22]. This contrasts with the findings of Mraiwa et al., who observed a diameter of up to 9.2 mm even in the absence of pathology [6]. Several studies revealed how gender and the presence of teeth affect anatomical features [6, 9, 11, 13, 17, 21]. It has been suggested that care should be taken with younger and female patients during surgical procedures due to root proximity to the MIC at the mid-root level of the maxillary central incisors [10, 12, 13, 23].

For evaluating the size and morphology of the MIC, various modalities have been employed and documented in the literature [5, 7–13, 20, 21]. Diagnostic imaging for the anterior maxilla has included two-dimensional (2-D) methods (intra-oral radiography and panoramic imaging) and cross-sectional or multiplanar-reformatted computed tomography (CT) [24]. The introduction of cone-beam computed tomography (CBCT) has opened up new diagnostic opportunities in dentistry [25]. Three-dimensional (3-D) imaging techniques allows a thorough anatomical examination within all three planes (axial, sagittal, and coronal) [7]. The MIC can be assessed using CT scans [6, 13, 17], micro-XCT images [11, 20], high resolution magnetic resonance imaging [26] and limited CBCT [9].

There is a data gap regarding African cohorts because previous studies on the anatomical features and size of the MIC have mostly focused on Western populations. To fill this gap, this study analysed the maxillary IC in a population of South Africans utilizing high-resolution micro-XCT imaging. Although a few studies have investigated age- and gender-related variations in MIC morphology, there aren't many thorough analyses that compare racial and gender characteristics. This study investigated these factors to better understand MIC architecture for improved surgical results and dental implant planning in different groups.

Clinical application

In the anterior maxilla, immediate implant placement is frequently chosen as a treatment option since it shortens recovery time and requires less surgical procedures [12, 27]. Despite its popularity, the protocol of immediate implant placement is still debatable, as it comes with a high risk of complications, especially when there is insufficient buccal and palatal alveolar bone [27, 28]. Implant failure might result when there is insufficient palatal bone with perforation into palatal soft tissues or MIC [23, 29]. A study by Alkanderi (2019) showed that approximately 8% of cases planned for immediate implant placement may perforate the maxillary IC [30]. It is well known that primary implant stability is one of the prerequisites for successful implant osseointegration [28, 31]. To achieve

primary stability during immediate implant placement, between 3 and 5 mm of bone is needed beyond the apex and toward palatal direction to place a dental implant of at least 10 mm in length [31]. Todorovic et al. (2023); concluded that although the alveolar bone on the palatal aspect was thicker compared to the buccal side, the crestal bone can present with dimensions less than 1 mm [27]. In the severely atrophied maxilla, surgical procedures such as MIC grafting and nerve displacement have been described, however these procedures are not commonly employed [4, 14, 23, 32–35]. A single, cylindrical maxillary IC appears to be the most suitable anatomic variation for such procedures [14]. Despite the fact that the majority of studies show no altered sensation following MIC grafting, the literature lacks comprehensive information on the dangers and clinical repercussions of harming the canal and its neurovascular structures (14, 23, 32–35). When the MIC is violated during oral surgical procedures like central incisor apicoectomies, enucleation of nasopalatine duct cysts, LeFort 1 osteotomies, surgically assisted rapid palatal expansion, and dental implant placement, it can result in surgical complications such as sensory dysfunction or non-osseointegration of implants [6, 7, 23].

Only a few studies have used micro-XCT to investigate the micro-anatomy of the MIC [11, 20]. Kim and associates reported on the usefulness of micro-XCT in analysing the internal microstructure of bones [29]. Micro-XCT has an imaging resolution of 5 μm at the maximum, making it possible to evaluate complex structural properties [29]. In our study, micro-XCT was utilized to quantify the maxillary IC dimensions, assess its anatomical properties, and determine the buccal wall dimensions of the MIC. This is the first instance of micro-XCT being employed for this function that we are aware of.

Materials and methods

Study design

This retrospective, cross-sectional study analysed and included existing data from 108 human cadaver skulls to examine the anatomical features of the MIC. This descriptive study provides detailed measurements and descriptions, and correlational as it explores the relationship between the anatomical features and sociodemographic variables such as gender and race.

Setting

The skeletal material was scanned at high resolution in the Micro-Focus X-ray Radiography and Tomography Facility (MIXRAD) of the South African Nuclear Energy Corporation, South Africa (NECSA) using a Nikon XTH 225 ST industrial Computed Tomography system (Nikon XTH 225 ST, Nikon Corporation, Japan).

Participants

Skeletal material (skulls) from the Pretoria Bone Collection have been used in this study. The research collection has a proud history that started in August 1942 [36, 37]. The skulls that were scanned were accessioned into the collection between 1990. and 2012. Upon arrival at the Department of Anatomy, an accession number was given to the deceased, which was recorded in the cadaver registry. This number was linked to the individual's personal details. The body was then embalmed and placed in storage for 1–2 years before dissection of the cadavers took place [36]. Following dissection, the cadavers were macerated and processed into skeletal elements [37]. The criterion for the skeletal remains to be included in the research collection, is that age, sex and population affinity of the individuals were known [36]. The skulls were then stored in acid-free cardboard boxes in temperature-controlled rooms to ensure their preservation and integrity.

The following were the inclusion criteria for this study: (a) Anatomically complete maxillary IC and surrounding maxillary bone, (b) presence of maxillary central incisors and (c) available demographic information. The exclusion criteria were (a) impacted teeth in the region of interest, (b) presence of a radiolucent, radiopaque, or mixed radiolucent-radiopaque lesion in the region of interest; (c) dental implants or bone grafts in the region of interest. Additionally, the patients' edentulous status was noted and excluded when the central incisors were missing in this study, which may have an effect on the anatomical structure due to maxillary resorption.

Sociodemographic variables were categorized into two groups: gender (male/female) and population (Black/White).

Measurements

For each skeletal element the best scanning parameters were selected according to the size and the density of the bone. Due to the specimen size in this study, a spatial resolution of less than 90 microns for the respective tomograms of the maxillae were achieved. This resulted in a much higher quality tomogram (3-D image) than CBCT from which more accurate quantitative analyses could be made [38]. Each of the 2-D digitized radiographs per specimen, taken at different angles, consisted of an array of 2048 \times 2048-pixel elements (maximum for the current detector at the micro-XCT device) and each element with a 16-bit gray scale (65535 Gy levels). The reconstruction into 2-D slices (for each row of the 2048 \times 2048-pixel array), was performed through Nikon CT-Pro 3-D software, a commercial tomography reconstruction package for micro-XCT, which created a single virtual 3-D volume file by reconstructing all the 2-D slices together with all the information of the sample.

The volume files were imported into advanced volume rendering software (VGStudio MAX 2.2, Volume Graphics GmbH, Germany) for the 3-D rendering, segmentation, and visualisation of the reconstructed volume data. The software offers quantitative analysis of the virtual volume and a menu of analytical functions is available, so that distances in 3-D space can be measured by integrating the information provided by the 3-D image together with the axial, sagittal and coronal views which show the additional xy, yz and xz slices, respectively. The specimen is defined through a density map of constituents of the sample as the virtual volume is being defined by 3D voxel elements, each with a different voxel value representing its density (up to 56535 Gy values), enabling the possibility of porosity quantification throughout the sample.

Evaluation of images

The Frankfort horizontal plane was created on the 3-D model as a line approximating the base of the cranium, passing from the infraorbital ridge to the midline of the occiput, intersecting the superior margin of the external auditory meatus. This allowed for the cranium to be in the anatomic position where the base of the skull lies in the correct horizontal plane and where right and left sides are level. A repeatable reference plane allowed us to orientate all skulls in a similar manner from which measurements could be taken.

Anatomical characteristics of the IC

Coronal and sagittal views were used to evaluate the anatomic characteristics of the MIC. In sagittal slices, the anatomic variants of the MIC were classified into four groups: [1] cylinder-shaped; [2] funnel-shape; [3] banana-shaped and [4] hourglass-shaped, in accordance with Mardinger and Mraiwa classifications [6, 13]. In coronal slices, the anatomic variants of the MIC were classified into three groups according to Bornstein's proposed classification (2011): [1] a single canal; [2] two parallel canals and [3] variations of the Y-type canal with one oral opening (ICO) and two or more nasal openings (ICN) [9].

Measurements to determine dimensions of the IC

The dimensions of the MIC were measured in millimetre, to the second decimal. Measurements were taken using all three anatomical planes (axial, sagittal and coronal). The following landmarks were selected for standardized measurements [1] the diameter of the foramina of Stenson (ICN) was measured at the level located on the axial plane where the ICN was at its largest (when two or more nasal openings were present, the diameters of all nasal openings were added together and a mean value was calculated); [2] diameter of the incisive foramen (ICO) was measured at the level located on the axial plane when the incisive foramen of the MIC was at its largest (when

more than one oral opening was present, the diameters of all openings were added together, and the mean value was calculated); [3] MIC length (ICL) was defined as the distance from the ICO to the ICN. When two parallel canals or canals with a Y-shaped morphology were present, the length was calculated as a mean value of the different canal measurements.

Measurements to determine dimensions of the buccal bone wall in relation to the IC

[4] The most crestal measurement (ICABC) evaluated the distance from the buccal border of the ICO to the facial aspect of the buccal bone plate; [5] the second measurement was taken at the level opposite the palatal border of the ICO to the facial buccal bone wall (ICABM); [6] the most cranial (apical) reading (ICABA) evaluated the distance from the buccal border in the middle of the IC to the facial aspect of the buccal bone wall; [7] the height of the buccal alveolar bone (ICABH) was measured as follows: a line was drawn from the ICN to the most prominent point of the nasal spine. A second line was drawn perpendicular to this line and extended to the most coronal point of the alveolar crest. All measurement performed in sagittal view are displayed in Fig. 1.

The ICO's distances in the axial plane to the roots of teeth #11 and #21 were measured. The slices were assessed in an apical to coronal direction. The measurement was made at the point at where the ICO's diameter was at its largest, which was usually 0–3 mm below the crestal bone of tooth #11 or #21. The measurement was specifically collected from the location on the palatal aspect of tooth #11 or tooth #21 that was closest to the ICO (see Fig. 2).

Reliability of measurements

Reliability of the measurements was performed by re-evaluating randomly 10% of samples twice after one-week interval and without any knowledge of previous measurements. In cases where discrepancies arose, a third evaluator was involved until adequate calibration was achieved. Intra-class correlation coefficients of 0.97 were achieved showing reproducibility of the evaluation of the categorical data. A kappa figure of 0.92 was achieved when comparing the numerical data, again showing good reliability of results obtained.

Sample size

The practical limitations and past research precedents were taken into consideration when determining the sample size for this study. One hundred and twenty-three (123) human cadaver skulls were scanned using extremely accurate micro-XCT imaging. Following the application of stringent inclusion criteria, 15 skulls were eliminated, leaving 108 skulls in the final sample. The quantity of

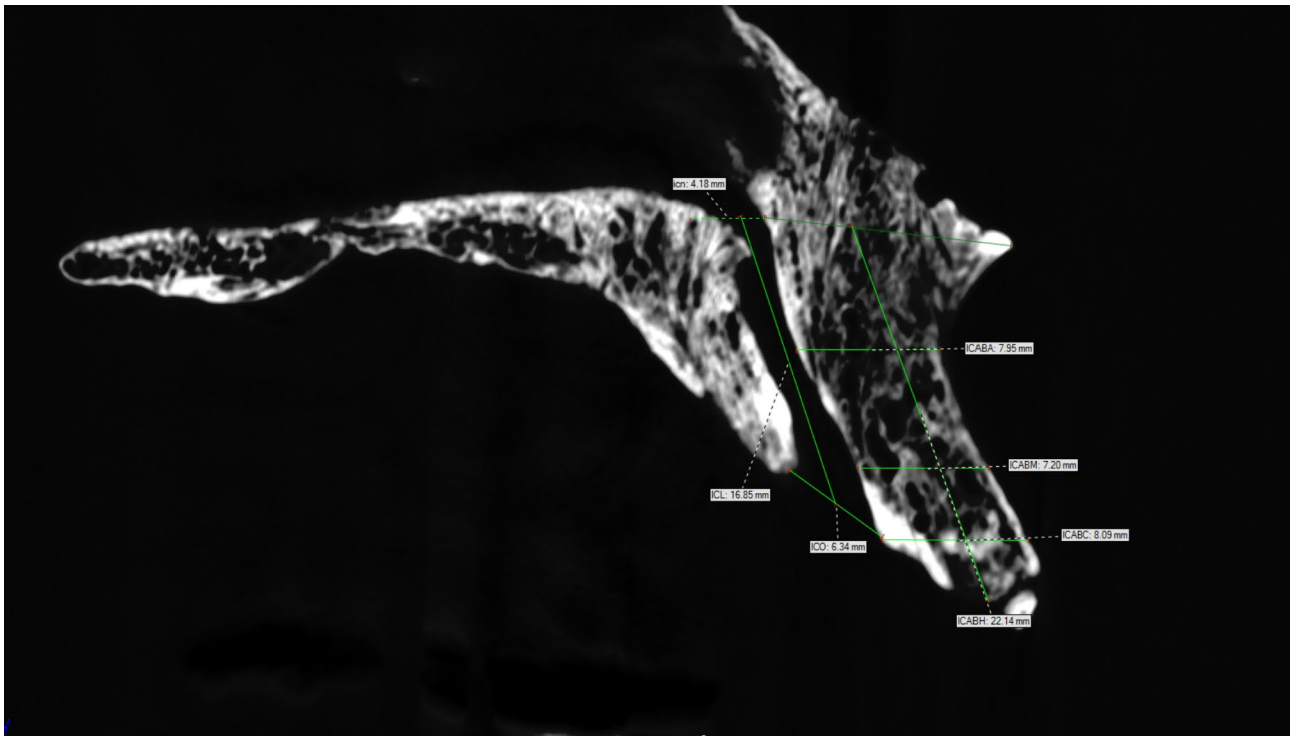


Fig. 1 All measurement performed in sagittal view



Fig. 2 A measurement of the closest position of tooth #11/#21 on the palatal aspect to the ICO (Occlusal view)

acceptable skulls available for scanning and the restricted scan time available, determined the selection of this sample size. Furthermore, most cited studies have employed comparable sample sizes, which guarantees conformity with accepted research procedures. The high-resolution data from micro-CT, despite the small sample size, offers a solid foundation for further investigation and allows for

in-depth anatomical understanding that can guide larger-scale studies.

Ethics approval was obtained from the Human Research Ethics Committee of the Faculty of Health Sciences, University of Pretoria, South Africa (No. 111/2013) and the Helsinki Declaration was signed.

Table 1 Demographic data

Population and gender	n	Average age (in years)
Black male	37	46.95 (± 15.68)
Black female	19	39.42 (± 15.66)
White male	26	63.35 (± 15.28)
White female	26	66.69 (± 14.51)
Total	108	54.10 (± 18.53)

Statistical analysis

Statistical Analysis System (SAS 9.4) was used to conduct the statistical analyses. Descriptive statistics were calculated on all the variables in the analysis according to the different population and gender classifications of interest in this study. In order to compare mean measurement differences between multiple groups the non-parametric alternative to an Analysis of Variance (ANOVA) was considered, namely the Kruskal-Wallis test, due to the non-normality of the data. The non-parametric alternative to

pairwise comparisons between different groups, namely the Dwass-Steel-Critchlow-Fligner (DSCF) test was also used to determine between which groups the mean differences were detected.

Results

The mean age of the population was 54.48 years (SD:18.53; SE:1.79; 95% CI: 50.92–58.03(*n*=108)) with 58.33% (*n*=63) being male and 41.67% (*n*=45) being female; and 48.15% (*n*=52) being white and 51.85% (*n*=56) being black. Demographic data of the subjects included in the study are displayed in Table 1.

The mean diameter of the ICO was 6.61 mm, while the ICL varied from 4.96 to 20.10 mm. The mean distances from teeth #11 and #21 to the ICO, were 1.88 and 1.83 mm, respectively. Table 2 shows the detailed descriptive analysis of all measurements performed across population groups and gender.

Table 2 Descriptive statistics based on measurements across population groups and gender

PopGen	Variable	N	Mean	Std Dev	25th Pctl	Median	75th Pctl	Std Error	Lower 95% CL for Mean	Upper 95% CL for Mean	Skewness	Kurtosis	Minimum	Maximum
Black Female	ICO	19	6.78	1.78	5.63	6.61	7.57	0.41	5.90	7.62	1.18	3.36	3.58	12.00
	ICL	19	12.59	1.98	10.97	12.74	13.70	0.46	11.63	13.54	0.59	0.73	9.48	17.51
	ICN	19	3.82	1.66	2.17	3.46	5.21	0.38	3.02	4.62	0.26	-1.30	1.57	6.67
	ICABC	19	6.30	1.12	5.51	6.54	7.11	0.26	5.76	6.84	-0.32	-0.52	4.17	8.33
	ICABM	19	6.56	1.18	5.84	6.66	7.54	0.27	5.99	7.13	-0.26	-0.42	4.34	8.47
	ICABA	19	7.58	1.59	6.52	7.65	8.83	0.37	6.82	8.35	0.26	-0.65	5.02	10.61
	ICABH	19	21.68	3.42	19.91	21.01	23.76	0.78	20.04	23.33	0.68	1.46	15.26	30.45
	OIC11	19	1.66	0.51	1.37	1.66	1.88	0.12	1.42	1.91	0.29	0.34	0.68	2.71
	OIC21	19	1.78	0.76	1.25	1.71	2.33	0.17	1.42	2.15	0.48	-0.62	0.75	3.37
Black Male	ICO	37	6.47	1.53	5.55	6.42	7.18	0.25	5.96	6.98	0.63	0.96	3.38	10.88
	ICL	37	11.79	3.35	9.91	11.70	13.99	0.55	10.67	12.90	0.26	0.32	4.96	20.10
	ICN	37	3.99	1.78	2.64	3.85	5.12	0.29	3.40	4.58	0.34	-0.76	1.26	7.65
	ICABC	37	6.80	1.46	5.82	6.69	7.74	0.24	6.31	7.28	0.15	1.41	3.05	10.90
	ICABM	37	7.03	1.69	5.73	7.13	8.15	0.28	6.47	7.59	0.44	0.94	3.28	11.89
	ICABA	37	7.50	2.18	5.90	7.52	8.38	0.36	6.77	8.22	0.77	1.41	3.35	13.52
	ICABH	37	21.01	3.08	19.30	20.37	23.09	0.51	19.99	22.04	0.17	-0.39	14.47	27.17
	OIC11	37	1.83	0.92	1.25	1.74	2.34	0.15	1.53	2.14	2.01	7.14	0.40	5.63
	OIC21	37	1.81	0.89	1.27	1.67	2.01	0.15	1.52	2.11	2.76	11.31	0.84	5.86
White Female	ICO	26	6.53	1.54	5.38	6.47	7.74	0.30	5.91	7.15	0.17	-0.45	3.58	9.97
	ICL	26	10.91	2.64	8.86	10.90	12.98	0.52	9.84	11.97	0.10	-0.84	6.18	15.93
	ICN	26	3.70	1.29	2.94	3.72	4.24	0.25	3.18	4.22	0.12	-0.16	1.04	6.15
	ICABC	26	6.53	1.18	5.79	6.32	6.98	0.23	6.05	7.00	1.01	0.89	4.71	9.36
	ICABM	26	6.85	1.33	5.89	6.48	7.61	0.26	6.31	7.38	0.84	0.73	4.42	10.23
	ICABA	26	7.62	1.28	6.68	7.51	8.44	0.25	7.11	8.14	0.84	1.02	5.82	11.22
	ICABH	26	18.94	2.18	16.88	19.19	20.41	0.43	18.06	19.82	0.02	-0.59	15.02	23.33
	OIC11	26	1.88	1.00	1.19	1.81	2.29	0.20	1.48	2.29	0.74	0.27	0.42	4.39
	OIC21	26	1.94	0.98	1.33	1.70	2.41	0.19	1.55	2.34	0.68	-0.10	0.45	4.25
White Male	ICO	26	6.79	1.58	5.60	6.65	7.58	0.31	6.15	7.43	0.91	1.16	4.72	11.27
	ICL	26	11.38	3.10	9.45	11.31	13.81	0.61	10.13	12.64	0.04	-0.83	5.98	16.85
	ICN	26	4.41	2.66	2.93	3.71	4.33	0.52	3.33	5.48	2.65	6.85	2.26	13.36
	ICABC	26	6.94	0.97	6.35	7.14	7.73	0.19	6.55	7.33	-1.09	1.72	4.03	8.29
	ICABM	26	7.24	1.17	6.53	7.16	7.84	0.23	6.76	7.71	-0.32	2.35	3.86	9.84
	ICABA	26	7.95	1.49	6.98	8.01	9.03	0.29	7.35	8.55	-0.47	-0.00	4.70	10.32
	ICABH	26	19.26	2.98	16.89	18.91	21.68	0.58	18.06	20.46	0.19	-0.52	13.72	25.94
	OIC11	26	1.89	0.77	1.45	1.78	2.55	0.15	1.58	2.20	0.31	-0.60	0.52	3.35
	OIC21	26	1.97	0.69	1.61	1.82	2.38	0.14	1.70	2.25	-0.21	0.35	0.23	3.11

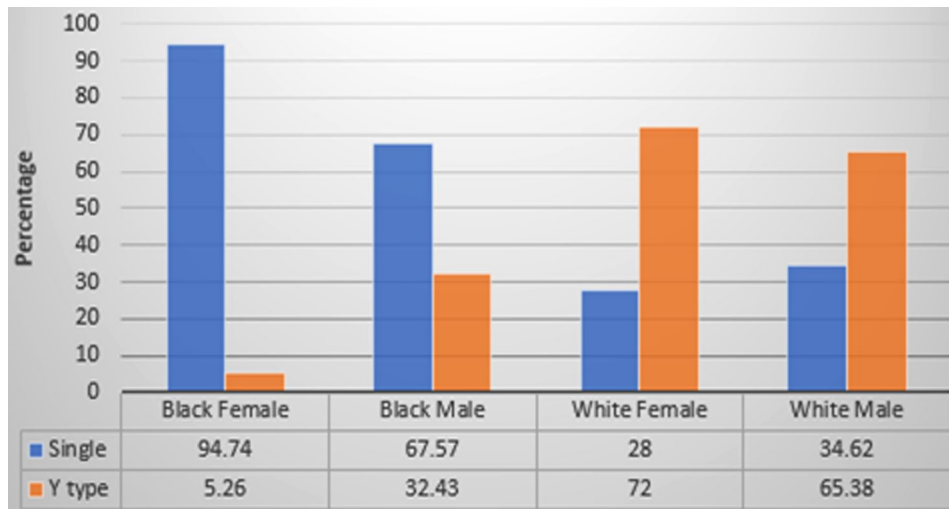


Fig. 3 Distribution of different IC types between population groups by gender in coronal view Note: One category in coronal view (2-parallel canals) was excluded from this part of the analysis since only one skull (white female) exhibited this characteristic (n = 108)

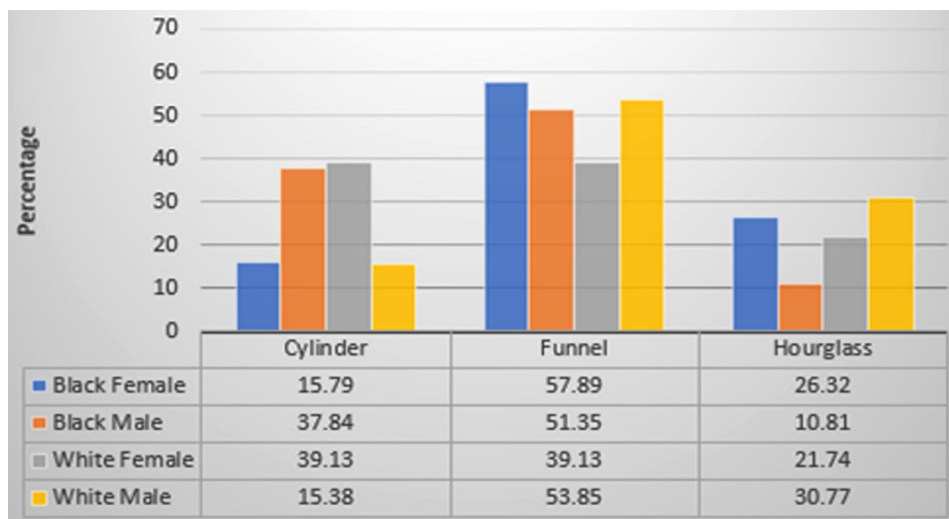


Fig. 4 Distribution of different IC types between population groups by gender in sagittal view. Note: One category in sagittal view (Banana shaped) were excluded from this part of the analysis since only three skulls (white female) exhibited this characteristic (n = 105)

Variables between population groups and genders for palatal bone measurements of OIC11 and OIC21 did not demonstrate significant differences. An interesting finding was that in 12.96% and 12.04% of cases for OIC11 and OIC21 respectively, the palatal bone was 1 mm or less from the maxillary IC.

When considering a possible relationship between population group by gender and different coronal views, namely Single canal and Y Type canal, there is very strong statistical evidence (Chi-square=26.226, df=3, $p < 0.0001$) to suggest that the coronal view is dependent on specific population and gender groups. Based on the coronal view a single canal being more prevalent in the black population and a Y-shaped canal being more prevalent in the white population (see Fig. 3).

In Fig. 3 it can be seen that 94.74% of the black female skulls (18 out of the 19 skulls) and 67.57% of the black male skulls (25 out of 37 skulls) had a single canal from the frontal view, whereas 72% of white female skulls (18 out of 25 skulls) and 65.38% of white male skulls (17 out of 26 skulls) had a Y type canal from the frontal view.

When considering a possible relationship between population group by gender and different sagittal views, namely cylinder, funnel and hourglass, there is no significance (Chi-square=8.816, df=6, $p = 0.1842$), suggesting that the sagittal view is not dependent on gender or population group (see Fig. 4).

When considering the ICABH and considering whether there are significant differences in this measurement across population groups and gender, it was

found there is sufficient statistical evidence to suggest that there are differences in these measurements (Chi-square=12.8228, $df=3$, $p=0.005$). Differences in ICABH measurements were found between black females and white females ($p=0.0134$) and also between black males and white females ($p=0.0414$). These results are presented in Table 3.

Discussion

This study provides a thorough investigation of the anatomical features of the MIC in a South African population using micro-XCT. The high-precision micro-XCT is a superior imaging modality in comparison to conventional medical cone-beam computed tomography (CBCT) [38]. Both imaging modalities are based on the same principle, except the spatial resolution obtained is shifted to 1–3 microns (μm) with micro-XCT instead of 300 μm with CBCT. To obtain a high quality three-dimensional (3-D) virtual image at this high spatial resolution, the number of 2-D projections (radiographs taken in 360° of the sample) increases from 375 to up to 8 000 projections (1 000 projections for this study).

The cohort, which had 108 skulls with a mean age of 54.48 years, was divided into four racial and gender groups: 36 black males, 19 black females, 26 white males, and 26 white females. The breakdown of the population by age showed that the majority of black women were under thirty, black men were between forty and fifty, white women were over sixty, and white men were over seventy. Age-related variations in canal diameters are important because they affect how dental implants are placed and how other surgical procedures are carried out in the anterior maxilla. In our study, for example, younger people, especially those under thirty, typically have shorter canals. According to Bains (2023), age has a substantial impact on the MIC diameter, with mean values often rising with age [39]. This may have an impact on the size of implant used and the requirement for further grafting surgeries. Studies by Bornstein [9], Fernandez-Alonso [4], and Salemi F [15] have demonstrated that the success of dental implants and other surgical procedures may be impacted by age-related morphological changes

in the MIC. These findings emphasize how crucial it is to take age-specific anatomical variations into account in order to maximize surgical success and reduce risks. For example, Bornstein [9] showed that diminished bone quality and greater bone resorption in older individuals increase the likelihood of implant failure, highlighting the necessity for customized surgical techniques. Age-related differences in canal dimensions support age-specific therapeutic considerations, as shown by our findings about gender variations in canal dimensions are consistent with those of Guncu [21] and Fernandez-Alonso [4], underscoring the need for surgical techniques tailored to each patient's gender.

The analysis showed that the ICL had an overall span of 4.96 to 20.10 mm and a mean of 11.62 mm. These measurements highlight the substantial variation in ICL and are consistent with earlier research by Song [11], Bornstein [9], Guncu [21], Tozum [10], Fukuda [20], and Salemi [15]. However, significant gender-based variations in ICL, as proposed by Gonul [7], Fernandez-Alonso [4, 5], Bains [39] and Panda [8], were not supported by our results. Our findings showed ICO mean diameter to be 6.61 mm (range 3.38–12.00 mm). This value is slightly bigger than that reported by Mraiwa [6], Bornstein [9], Fukuda [20], and Salemi [15], and it is consistent with observations made by Gonul [7]. In the present study, an average ICN diameter was 3.90 mm (range 1.04–12.15 mm), which is less than that reported by Mraiwa [6] and Al-Amery [12], but similar to that of Bornstein [9] and Panda [8].

Our study found that the thickness of the alveolar bone anterior to the canal varied from 6.69 mm at the most coronal region to 7.65 mm at the most apical area, in accordance with the findings of Mraiwa [6], Bornstein (2011) [9], Tozum [10], and Al-Amery [12]. In particular, Mraiwa found a range of 2.9–13.6 mm for bone thickness, with a mean value of 7.4 mm [6]. The alveolar bone thickness measured by Bornstein was 7.6 mm at the apical part, 6.59 mm at the midsection, and 6.5 mm at the crestal area [9]. Tozum measured the thickness of the bone at the crestal portion (5.62 mm), the midsection (6.68 mm), and the most apical portion (9.19 mm) [10]. Al-Amery found the nasal spine's thickest alveolar bone measured 10.75 mm, while the labial alveolus has the narrowest, measuring 5.7 mm, with an average thickness of 7.63 mm [12]. Furthermore, it was observed that the alveolar bone was often thicker in males [9, 10, 12]. It was also confirmed by Al-Amery [12] and Panda [8] that the thickness was higher in younger individuals. The mean height of the buccal alveolar bone was 20.21 mm (range 13.72–30.45 mm), which is significantly higher than Fukuda's [20] findings. There were also significant disparities between black and white females, as well as black males and females.

Table 3 ICABH measurements comparison within population groups and gender

Population/Gender	Wilcoxon Z	DSCF Value	Pr> DSCF
Black Female vs. Black Male	0.7182	1.0157	0.8899
Black Female vs. White Female	3.0220	4.2737	0.0134*
Black Female vs. White Male	2.2061	3.1199	0.1215
Black Male vs. White Female	2.6387	3.7316	0.0414*
Black Male vs. White Male	2.0733	2.9321	0.1618
White Female vs. White Male	-0.3752	0.5306	0.9820

The Dwass, Steel, Critchlow-Fligner method for pairwise comparison

p-value<0.05 denoted by *

The axial view distances from teeth #11 and #21 to the ICO, which were not disclosed in previous studies, revealed mean distances of 1.88 and 1.83 mm, respectively, indicating the crucial proximity of tooth sockets to the IC for anterior zone implant procedures. This is especially important when considering immediate implant placement to replace central incisors. In these cases, the drill is oriented more toward palatal to achieve sufficient primary stability and to stay away from engaging the buccal bone wall and may interfere with content of MIC. Our findings revealed that #21 and #11 tooth sockets are located in close proximity to important anatomical structures and highlighted the necessity for clinicians to use sophisticated imaging methods and perhaps guided implant placement procedures to reduce the risk of complications.

Our study identified clear associations between demographic factors and the MIC morphological features, especially regarding shape and prevalence in various coronal and sagittal perspectives. The analysis of coronal views showed the single canal shape to be more prevalent in the black population, while the white individuals were more likely to exhibit the Y-type canal. This finding is consistent with the studies by Gonul et al. [7] and Salemi et al. [15], which found that single-type canals were more common than Y-type canals. On the other hand, Fernandez Alonso et al. [3] found that Y-type canals were more common. Analysis in the sagittal plane revealed that the funnel form, which is found in all analysed demographic groups, is the most frequently encountered morphology of the MIC, followed by the cylindrical type. This distribution is consistent with findings published by Arnaut [40] and Fukuda et al. [20]. It does, however differ from the results of studies conducted by Tozum et al. [10], Guncu [21], and Gonul et al. [7], which reported a higher prevalence of cylindrical canal form. Because the MIC morphology varies so much, customized surgical planning is vitally important. This is particularly relevant to implant therapy in the anterior maxilla, where each patient's unique anatomy must be considered when deciding whether to pursue MIC augmentation.

Our research offers novel information on the structural differences of the MIC in a South African community in addition to validating earlier findings. These results highlight the importance of tailored surgical planning that considers each patient's unique anatomical differences in order to guarantee the best possible results for oral surgical treatments. Expanding the understanding of these anatomical traits in a variety of population groups should be the main goal of future research in order to improve clinical practice in oral surgery and implant dentistry.

Study limitations

The study has several limitations, including a relatively small sample size of 108 human cadaver skulls, which restricts the application of the findings, suggesting the need for larger, more diverse studies. The focus on only two South African demographic groups further limits the applicability to other ethnic or racial populations. We acknowledge that age is a potential confounding factor in our study, given the nearly 20-year age difference between black and white groups. While we observed anatomical variations may be influenced by ethnicity, we recognize that some of these differences might also be attributed to the age disparity. Correlation but not causation may be established with the retrospective cross-sectional design, and a prospective longitudinal approach could offer deeper insights. Although micro-XCT scanning provides high-resolution pictures, it is resource-intensive it may not fully replicate in vivo conditions, highlighting the need for complementary imaging methods like CBCT. Clinically significant anatomical changes may have been overlooked due to the omission of skulls with specific diseases. Therefore, in order to enhance comprehension and therapeutic relevance, additional research involving bigger and more varied sample sizes is required, particularly in complex cases to provide stronger guidance for dental practitioners.

Conclusion

This work offers a thorough analysis of the structural features and dimensions of the MIC using micro-XCT analysis of a South African cohort, revealing notable differences between demographic groups and genders. The study emphasizes that there are notable differences in the ICL and angulation, with males typically having longer canals than females. Additionally, it clarifies the intricate structure of the MIC by highlighting how near the central incisor sockets (#11 and #21) are—an average distance of less than 2 mm was found. These results imply that some demographic groups have a higher risk of surgical problems after dental implant surgeries. It emphasizes the significance of thorough preoperative evaluations using cutting-edge 3-D imaging technologies as it is the first study to our knowledge to take such detailed measurements from these tooth sockets. In order to minimize potential issues and improve the success of dental implants, it is imperative to customize surgical techniques based on the patient's unique anatomical traits. This is particularly important when considering immediate implant placements in the demanding anterior maxillary region.

Abbreviations

IC	Incisor canal
Micro-XCT	Micro-focus X-ray Computed Tomography
ICN Measurement	The diameter of the foramina of Stenson

ICO Measurement	The diameter of the incisive foramen
ICL Measurement	The incisive canal length defined as the distance from the incisive foramen to the foramina of Stenson
ICABC Measurement	The distance from the buccal border of the incisive foramen to the facial aspect of the buccal bone plate
ICABM Measurement	The measurement taken at the level opposite the palatal border of the incisive foramen to the facial buccal bone wall
ICABA Measurement	The distance from the buccal border in the middle of the incisive canal to the facial aspect of The buccal bone wall
ICABH measurement	The height of the buccal alveolar bone
OIC11 Measurement	The distance from the incisive foramen to the tooth #11
OIC21 Measurement	The distance from the incisive foramen to the tooth #21
CEJ	Cemento-enamel junction

Author contributions

VST: design of the study, measurements of the sample, data sheets, monitoring of the study development, corrections of the draft before submission, approval of the manuscript for submission and submission procedure. MMB: measurements of the sample, interpretation of data, data sheets, writing up the manuscript, approval of the manuscript for submission. JK: statistical analysis of the data, interpretation of data, approval of the manuscript for submission. JH: preparation of the study sample, corrections of the draft before submission, approval of the manuscript for submission. AWZ: conceiving the idea, design of the study, monitoring of the study development, corrections of the draft before submission, and approval of the manuscript for submission.

Funding

The study was partially supported by the research grant No. 660-01-0009/2023-03/6 of the Ministry of Science, Technological Development and Innovation of the Republic of Serbia.

Data availability

The data that support the findings of this study are not openly available due to reasons of sensitivity and are available from the corresponding author upon reasonable request.

Declarations

Ethics approval and consent to participate

Ethics approval was obtained from the Research Ethics Committee of the Faculty of Health Sciences, University of Pretoria, South Africa (No. 111/2013) and the Helsinki Declaration was signed. Consent to Participate declaration: not applicable.

Consent for publication

Not applicable.

Competing interests

The authors declare no competing interests.

Received: 14 June 2024 / Accepted: 11 October 2024

Published online: 18 October 2024

References

- Sferlazza L, Zaccheo F, Campogrande ME, Petroni G, Cicconetti A. Common anatomical variations of neurovascular canals and Foramina relevant to oral surgeons: a review. *Anatomia*. 2022;1(1):91–106.
- Żytkowski A, Tubbs RS, Iwanaga J, Clarke E, Polguy J, Wysiadecki G. Anatomical normality and variability: historical perspective and methodological considerations. *Translational Res Anat*. 2021;23:100105.
- Fernández-Alonso A, Suárez-Quintanilla J, Rapado-González O, Suárez-Cunheiro MM. Morphometric differences of nasopalatine canal based on 3D classifications: descriptive analysis on CBCT. *Surg Radiol Anat*. 2015;37:825–33.
- Fernández-Alonso A, Antonio Suárez-Quintanilla J, Muínelo-Lorenzo J, Varela-Mallou J, Smyth Chamosa E, Mercedes Suárez-Cunheiro M. critical anatomic region of nasopalatine canal based on tridimensional analysis: cone beam computed tomography. *Sci Rep*. 2015;5(1):12568.
- Fernández-Alonso A, Suárez-Quintanilla J, Muínelo-Lorenzo J, Bornstein MM, Blanco-Carrión A, Suárez-Cunheiro M. Three-dimensional study of nasopalatine canal morphology: a descriptive retrospective analysis using cone-beam computed tomography. *Surg Radiol Anat*. 2014;36:895–905.
- Mraiwa N, Jacobs R, Van Cleynenbreugel J, Sanderink G, Schutyser F, Suetens P, et al. The nasopalatine canal revisited using 2D and 3D CT imaging. *Dento-maxillofacial Radiol*. 2004;33(6):396–402.
- Gönül Y, Bucak A, Atalay Y, Beker-Acay M, Çalişkan A, Sakarya G, et al. MDCT evaluation of nasopalatine canal morphometry and variations: an analysis of 100 patients. *Diagn Interv Imaging*. 2016;97(11):1165–72.
- Panda M, Shankar T, Raut A, Dev S, Kar AK, Hota S. Cone beam computerized tomography evaluation of incisive canal and anterior maxillary bone thickness for placement of immediate implants. *J Indian Prosthodontic Soc*. 2018;18(4):356.
- Bornstein MM, Balsiger R, Sendi P, Von Arx T. Morphology of the nasopalatine canal and dental implant surgery: a radiographic analysis of 100 consecutive patients using limited cone-beam computed tomography. *Clin Oral Implants Res*. 2011;22(3):295–301.
- Tözüm TF, Güncü GN, Yıldırım YD, Yılmaz HG, Galindo-Moreno P, Velasco-Torres M, et al. Evaluation of maxillary incisive canal characteristics related to dental implant treatment with computerized tomography: a clinical multicenter study. *J Periodontol*. 2012;83(3):337–43.
- Song W-C, Jo D-I, Lee J-Y, Kim J-N, Hur M-S, Hu K-S, et al. Microanatomy of the incisive canal using three-dimensional reconstruction of microCT images: an ex vivo study. *Oral Surg Oral Med Oral Pathol Oral Radiol Endodontology*. 2009;108(4):583–90.
- Al-Amery SM, Nambiar P, Jamaludin M, John J, Ngeow WC. Cone beam computed tomography assessment of the maxillary incisive canal and foramen: considerations of anatomical variations when placing immediate implants. *PLoS ONE*. 2015;10(2):e0117251.
- Marding O, Namani-Sadan N, Chaushu G, Schwartz-Arad D. Morphologic changes of the nasopalatine canal related to dental implantation: a radiologic study in different degrees of absorbed maxilla. *J Periodontol*. 2008;79(9):1659–62.
- Peñarocha M, Carrillo C, Uribe R, García B. The nasopalatine canal as an anatomic buttress for implant placement in the severely atrophic maxilla: a pilot study. *Int J Oral Maxillofac Implants*. 2009;24(5):936–42.
- Salemi F, Atarbash Moghadam F, Shakibai Z, Farhadian M. Three-dimensional assessment of the nasopalatine canal and the surrounding bone using cone-beam computed tomography. *J Periodontology Implant Dentistry*. 2018;8(1):1–7.
- Von Arx T, Lozanoff S, Sendi P, Bornstein MM. Assessment of bone channels other than the nasopalatine canal in the anterior maxilla using limited cone beam computed tomography. *Surg Radiol Anat*. 2013;35:783–90.
- Liang X, Jacobs R, Martens W, Hu Y, Adriaenssens P, Quirynen M, et al. Macro- and micro-anatomical, histological and computed tomography scan characterization of the nasopalatine canal. *J Clin Periodontol*. 2009;36(7):598–603.
- Sicher H. Anatomy and oral pathology. *Oral surgery, oral medicine. Oral Pathol*. 1962;15(10):1264–9.
- Chapple I, Ord R. Patent nasopalatine ducts: four case presentations and review of the literature. *Oral surgery, oral medicine, oral pathology*. 1990;69(5):554–8.
- Fukuda M, Matsunaga S, Odaka K, Oomine Y, Kasahara M, Yamamoto M, et al. Three-dimensional analysis of incisive canals in human dentulous and edentulous maxillary bones. *Int J Implant Dentistry*. 2015;1(1):1–8.
- Güncü GN, Yıldırım YD, Yılmaz HG, Galindo-Moreno P, Velasco-Torres M, Al-Hezaimi K, et al. Is there a gender difference in anatomic features of incisive canal and maxillary environmental bone? *Clin Oral Implants Res*. 2013;24(9):1023–6.
- Lake S, Iwanaga J, Kikuta S, Oskouian RJ, Loukas M, Tubbs RS. The incisive canal: a comprehensive review. *Cureus*. 2018;10(7).
- Artzi Z, Nemicovsky CE, Bitlitum I, Segal P. Displacement of the incisive foramen in conjunction with implant placement in the anterior maxilla without jeopardizing vitality of nasopalatine nerve and vessels: a novel surgical approach. *Clin Oral Implants Research: Novel Dev*. 2000;11(5):505–10.
- Harris D, Buser D, Dula K, Gröndahl K, Jacobs R, Lekholm U, et al. EAO guidelines for the use of diagnostic imaging in implant dentistry. *Clin Oral Implants Res*. 2002;13(5):566–70.

25. Harris D, Horner K, Gröndahl K, Jacobs R, Helmrot E, Benic GI, et al. EAO guidelines for the use of diagnostic imaging in implant dentistry 2011. A consensus workshop organized by the European Association for Osseointegration at the Medical University of Warsaw. *Clin Oral Implants Res.* 2012;23(11):1243–53.
26. Jacob S, Zelano B, Gungor A, Abbott D, Naclerio R, McClintock MK. Location and gross morphology of the nasopalatine duct in human adults. *Archives Otolaryngology–Head Neck Surg.* 2000;126(6):741–8.
27. Todorovic VS, Postma TC, Hoffman J, van Zyl AW. Buccal and palatal alveolar bone dimensions in the anterior maxilla: a micro-CT study. *Clin Implant Dent Relat Res.* 2023.
28. Chen ST, Buser D. Esthetic outcomes following immediate and early implant placement in the anterior maxilla—a systematic review. *Int J Oral Maxillofac Implants.* 2014;29(Suppl):186–215.
29. Kim JH, Lee JG, Han DH, Kim HJ. Morphometric analysis of the anterior region of the maxillary bone for immediate implant placement using micro-CT. *Clin Anat.* 2011;24(4):462–8.
30. Alkanderi A, Al Sakka Y, Koticha T, Li J, Masood F, Suárez-López Del Amo F. Incidence of nasopalatine canal perforation in relation to virtual implant placement: a cone beam computed tomography study. *Clin Implant Dent Relat Res.* 2020;22(1):77–83.
31. Bhole M, Neely AL, Kolhatkar S. Immediate implant placement: clinical decisions, advantages, and disadvantages. *J Prosthodontics: Implant Esthetic Reconstr Dentistry.* 2008;17(7):576–81.
32. Peñarrocha D, Candel E, Guirado JLC, Canullo L, Peñarrocha M. Implants placed in the nasopalatine canal to rehabilitate severely atrophic maxillae: a retrospective study with long follow-up. *J Oral Implantology.* 2014;40(6):699–706.
33. Raghoobar GM, den Hartog L, Vissink A. Augmentation in proximity to the incisive foramen to allow placement of endosseous implants: a case series. *J Oral Maxillofac Surg.* 2010;68(9):2267–71.
34. Rosenquist J, Nyström E. Occlusion of the incisal canal with bone chips. A procedure to facilitate insertion of implants in the anterior maxilla. *Int J Oral Maxillofac Surg.* 1992;21(4):210–1.
35. Scher EL. Use of the incisive canal as a recipient site for root form implants: preliminary clinical reports. *Implant Dent.* 1994;3(1):38–41.
36. L'Abbé E, Loots M, Meiring J. The Pretoria bone collection: a modern South African skeletal sample. *Homo.* 2005;56(2):197–205.
37. L'Abbé EN, Krüger GC, Theye CE, Hagg AC, Sapo O. The Pretoria bone collection: a 21st century skeletal collection in South Africa. *Forensic Sci.* 2021;1(3):220–7.
38. Hoffman JW, De Beer F, editors. Characteristics of the micro-focus x-ray tomography facility (MIXRAD) at Necsa in South Africa. 18th World Conference on Nondestructive Testing; 2012.
39. Bains SK, Bhatia A, Sodhi SS, Sharma A. Assessment of the Nasopalatine Canal in patients requiring Dental implants in the Maxillary Anterior Region using Cone Beam Computed Tomography. *Cureus.* 2023;15(12).
40. Arnaut A, Milanovic P, Vasiljevic M, Jovicic N, Vojinovic R, Selakovic D, et al. The shape of nasopalatine canal as a determining factor in therapeutic approach for orthodontic teeth movement—a CBCT study. *Diagnostics.* 2021;11(12):2345.

Publisher's note

Springer Nature remains neutral with regard to jurisdictional claims in published maps and institutional affiliations.